

# Linear Dynamics of End-Functionalized Polymer Melts: Linear Chains, Stars, and Blends

Dimitris Vlassopoulos,<sup>\*,†</sup> Marinos Pitsikalis,<sup>†,‡</sup> and Nikos Hadjichristidis<sup>†,‡</sup>

Foundation for Research and Technology-Hellas (FO.R.T.H.), Institute of Electronic Structure and Laser, P.O. Box 1527, 71110 Heraklion, Crete, Greece, and Department of Chemistry, University of Athens, Panepistimiopolis Zografou, 15771 Athens, Greece

Received April 28, 2000; Revised Manuscript Received August 21, 2000

**ABSTRACT:** We investigated the linear viscoelastic response of model mono-, di-, and tri- $\omega$ -functionalized three-arm star polybutadiene melts with zwitterionic end groups using dynamic rheological measurements. Depending on the degree of functionalization, these polymers self-assembled into distinct supramolecular structures resembling nonspherical starlike objects, transient networks consisting of highly branched structures, and collapsed soft-sphere conformations, with aggregation numbers affected by the arm molecular weight. The dependence of the relaxation times on the latter indicated activated processes analogous to multiarm star polymers. On the other hand, the dynamics of  $\omega$ -functionalized linear chains, forming clusters with tubular or bcc structures, was characterized by a much smaller energetic barrier. The use of different sample preparation protocols as well as binary blends involving stars demonstrated the stability of the self-organized structures and confirmed the assignment of the relaxation processes.

## 1. Introduction

The recent progress in the anionic synthesis of well-characterized telechelic polymers bearing functional end groups<sup>1</sup> has helped addressing the role of Coulombic interactions in ionic polymeric materials of different architectures. This issue is of prime importance for the molecular design and use of supramolecular structures with desired properties for specific applications.<sup>2</sup> In a recent paper we have shown that three-arm polymer stars bearing strong polar end groups in one, two, or all three arms exhibit a variety of mesoscopic structures and a respective rich dynamic response.<sup>3</sup>

Here we address the effects of arm molecular weight on the dynamics of these self-organized macromolecular objects and further compare the dynamics of these stars against that of  $\omega$ -functionalized linear chains of similar molecular weights. We also explore the stability of the various self-assemblies by using different sample preparation protocols or binary mixtures involving different telechelic stars of the same molecular weight or a star with a nonionic linear chain. Our results support the emerging picture suggesting that selective functionalization of the arms ends yields a variety of self-organized structures and respective dynamics much different from that of the nonfunctionalized precursor polymer, providing thus a means for supramolecular structural control. By demonstrating a smooth transition between the different constituent structures of the two components in a binary mixture when its composition is altered, we provide further indirect evidence of the assignment of the different relaxation modes and the stability of the structures.

## 2. Experimental Section

**Materials.** The anionic synthesis and characterization of linear  $\omega$ -zwitterionic and mono-, di-, and tri- $\omega$ -zwitterionic three-arm star symmetric (same molecular weight per arm) 1,4-polybutadienes are described in detail elsewhere.<sup>4</sup> Their

**Table 1. Molecular Characteristics of the  $\omega$ -Functionalized Three-Arm Star and Linear 1,4-Polybutadienes<sup>4</sup>**

sample	code from ref 4	$M_a$ (g/mol) <sup>a</sup>	$M_w/M_n$	$f$	$T_g$ (°C)
ZW1-15	Zw-1N-3PBd15	16 000	1.12	3.0	−84
ZW1-30	Zw-1N-3PBd30	37 500	1.07	3.0	−85
ZW1-40	Zw-1N-3PBd40	50 000	1.14	3.1	−88
ZW2-15	Zw-2N-3PBd15	14 500	1.07	3.1	−69
ZW2-30	Zw-2N-3PBd30	20 500	1.01	2.9	−82
ZW2-40	Zw-2N-3PBd40	32 500	1.11	2.8	−85
ZW3-15	Zw-3N-3PBd15	11 000	1.08	2.8	−71
ZW3-25	Zw-3N-3PBd25	23 500	1.08	2.7	−69
ZW3-40	Zw-3N-3PBd40	30 500	1.02	2.8	−81
ZW-L-20	ZW-L-20	20 500	1.02		−77
ZW-L-40	ZW-L-40	41 000	1.02		−79
ZW-L-75	ZW-L-75	80 500	1.03		−82

<sup>a</sup> Number-average arm molecular weight.

molecular characteristics, i.e., number-average arm molecular weight ( $M_a$ ), polydispersity ( $M_w/M_n$ ), functionality ( $f$ ), and glass transition temperature ( $T_g$ ), are summarized in Table 1. Samples ZW1, ZW2, and ZW3 refer to stars with one, two, or all three ends functionalized with zwitterionic groups, respectively, whereas samples ZW-L refer to the linear one end-functionalized chains. Before use the samples were annealed under vacuum at 70 °C for 12 h in order to eliminate any undesirable traces of humidity, because of the sensitivity of zwitterionic groups. In some cases annealing at the same conditions but over several (7) days was performed in order to ensure that the measurements were conducted under equilibrium for these materials, as discussed below. This important point was further confirmed by using samples obtained via solution casting, as discussed below.

Mixtures of different stars or a star with a nonfunctionalized linear 1,4-polybutadiene chain (with molecular weight 165 000 and polydispersity 1.05, coded as PB165) were investigated as well. More specifically, two blends were used: a star/linear blend of ZW3-15 and PB165, with weight compositions in star 0.2, 0.3, and 0.5; and a star/star blend of ZW2-15 and ZW3-15 with weight compositions in the latter 0.35 and 0.53. The various blend samples were prepared by mixing the two component dilute solutions (in toluene or cyclohexane as discussed below) and subsequently slowly evaporating the solvent over the course of 5 days under vacuum at room temperature (for cyclohexane) or 50 °C (for toluene). At the

<sup>†</sup> Institute of Electronic Structure and Laser.

<sup>‡</sup> University of Athens.

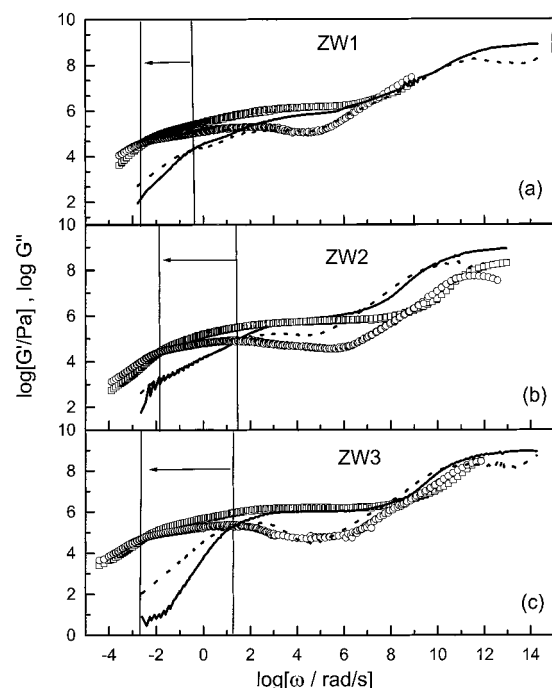


**Figure 1.** Master curves of elastic ( $G'$ ) and viscous ( $G''$ ) moduli at the reference temperature 27 °C for three-arm 1,4-polybutadiene stars with arm molecular weights 40 000 ( $G'$ ,  $\square$ ;  $G''$ ,  $\circ$ ) and 15 000 ( $G'$ , solid line;  $G''$ , dotted line), respectively (based on Table 1). (a) ZW1-40 and ZW1-15; (b) ZW2-40 and ZW2-15; (c) ZW3-40 and ZW3-15. The vertical lines indicate the crossover frequencies from rubber plateau to terminal relaxation, and the arrows show the effect of increasing arm molecular weight in slowing down the terminal relaxation.

end of this procedure the samples were annealed in the usual procedure.

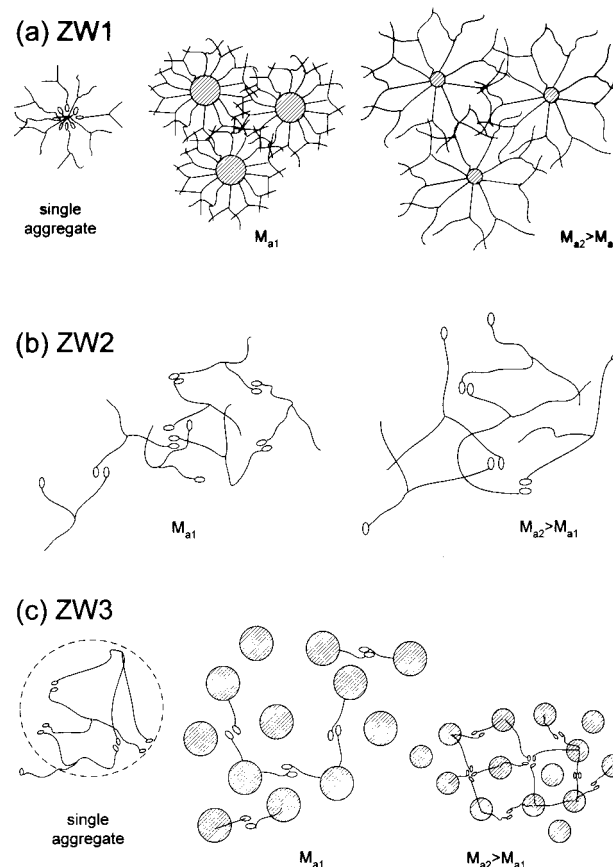
**Methods.** The linear dynamics of the various samples was investigated by means of small-amplitude oscillatory shear measurements (dynamic frequency sweeps) carried out with a Rheometric Scientific ARES 2KFR1N1 rheometer in the parallel plate geometry (diameter 8 mm, gap 1 mm,  $N_2$  gas convection temperature control) over a wide temperature range (−87 to 130 °C). Dynamic strain sweeps were also performed in order to determine the regime of linear viscoelasticity for the frequency sweeps.

The glass transition temperatures were obtained from differential scanning calorimetry measurements (DSC), which were carried out by using a Rheometric Scientific PL-DSC instrument with a heating/cooling rate of 10 °C/min.

### 3. Results and Discussion

Figure 1 depicts typical comparative moduli master curves obtained from dynamic frequency sweeps with reference temperature  $T_r = 27$  °C, for ZW1, ZW2, and ZW3 and two different arm molecular weights, the highest (about 40 000 g/mol) and the lowest (about 15 000 g/mol), as per Table 1. The behavior of the smaller stars is already established on the basis of the additional structural evidence from SAXS, as reported in ref 3. According to this, ZW1 stars form supramolecular self-assemblies resembling multiarm star-like dendrimers (see also Scheme 1a). ZW2 stars form transient networks consisting of highly branched structures with a very broad relaxation spectrum (Scheme 1b). ZW3 stars are predominantly organized into intramolecularly aggregated collapsed star conformations with soft-sphere behavior,<sup>5</sup> where limited partial branching of these spheres cannot be excluded (Scheme 1c).

**Scheme 1. Schematic Illustration of the Self-Organization of the Telechelic Three-Arm Stars of Different Molecular Weights<sup>a</sup>**



<sup>a</sup> (a) ZW1: one-arm end-functionalized. In this case only intermolecular associations are possible, leading to the formation of supramolecular dendritic stars. As the arm molecular weight ( $M_a$ ) increases, the cores representing the associating zwitterionic groups become smaller due to stereochemical reasons, and their distances are enhanced, with a larger network of interpenetrating nonfunctionalized arms. (b) ZW2: two arms end-functionalized. This yields the formation of a transient network, which is larger for higher  $M_a$ . (c) ZW3: all three arms end-functionalized. There is evidence of the tendency of stars to form collapsed soft-sphere configurations involving a few stars, some of which may have a free arm (depending on the aggregation number). The dotted circle around the cartoon of a single aggregate illustrates the consideration of such self-assemblies as spherical objects. Increasing  $M_a$  yields a transient network in equilibrium with spheres.

As is evident from Figure 1, increasing the arm molecular weight has a great impact in slowing the dynamics. The self-organization is presumably altered as the aggregation number should be affected by the size of the stars, primarily due to stereochemical reasons, as judged from dilute solution studies (it is reduced with increasing molecular weight).<sup>6,7</sup> However, from the dynamic information and the assignment of the relaxation processes (based on the available structural information<sup>3</sup>), it is possible to account for the molecular weight dependence of the relaxation times, as discussed below.

Referring to Figure 1a for ZW1, for which only intermolecular clusters are formed, the interaggregate distances are larger for the higher molecular weight stars, and thus these self-organized structures cannot be detected with SAXS; in fact, SAXS measurements on the ZW1-40 sample did not show any peak of the

scattering intensity over the available scattering wave-vector  $q$  range. Given the larger arm molecular weight of ZW1-40 compared to ZW1-15, the respective overall size of the clusters is larger, shifting the structural SAXS peak to lower (inaccessible)  $q$ 's and the dynamic response to much longer times (also inaccessible). An attempt to represent the self-assembly of ZW1 stars of different arm molecular weights is depicted in the cartoons of Scheme 1a.

Concerning the self-organized structures of the various end-functionalized polymers discussed here, a remark is in order. It is actually true that direct structural information would provide further support to the interpretation of the rheological data discussed in this section, as was the case for the low molecular weight samples in ref 3. However, in the present case of higher molecular weights SAXS measurements are not appropriate as already discussed. On the other hand, alternative scattering techniques such as light scattering and SANS are also not applicable here because of the virtual absence of the necessary contrast (refractive index increment and deuteration, respectively). We are thus left with a complete set of systematic rheological data that are interpreted in view of limited structural evidence,<sup>3</sup> relevant information from dilute solution studies,<sup>6</sup> and experimental and theoretical investigations on complex macromolecular systems exhibiting similarities, reported in the literature.

As evidenced from Figure 1, for the large stars the complete terminal relaxation cannot be detected by using frequencies as low as 0.01 rad/s and temperatures as high as 130 °C. One can however note the similarities in the dynamics of samples ZW*i*-15 and ZW*i*-40,  $i = 1, 2$ , or 3, and at the same time the distinct difference among the three groups. In particular, the increase in the number of dipolar groups (from mono- to di- to trifunctionalized stars) relates to a larger difference in the onset of terminal relaxation between ZW*i*-15 and ZW*i*-40. On the basis of Figure 1a, the rubber plateau region is extended toward the low frequencies, maintaining a broad maximum well separated from the  $G'$ – $G''$  crossover, and the onset of terminal relaxation is only reached at the lowest frequencies and highest temperatures probed.<sup>8</sup> The apparent molecular weight effect on the high-frequency Rouse-like regime, as evidenced from the change of the crossover frequency to the rubber plateau in Figure 1, is attributed to the change of  $T_g$  (and thus the segmental dynamics) with molecular weight, in addition to the dependence of classical Rouse modes. The  $T_g$  effect is rather significant as seen in Table 1 and is a result of the changing microstructure of polybutadiene (increase of 1,2-content) with functionalization for the different molecular weights,<sup>4,6c</sup> as well as the reduced concentration of stars (and thus of zwitterionic groups) with increasing molecular weight. Therefore, the shift of the high-frequency relaxations with molecular weight in Figure 1 is primarily explained by the faster segmental times of ZW*i*-40 compared to ZW*i*-15. This high-frequency region has three notable features: (i) The extended breadth of ZW1-15 (exceeding 3 decades), which relates to the specific self-organized structure and the reduced  $T_g$  compared to ZW2-15 and ZW3-15.<sup>3</sup> We have compared the behavior of ZW1-15 with the respective high-frequency response of a multiarm polybutadiene star with  $f = 64$  arms and arm molecular weight  $M_a = 7000$  g/mol and  $T_g = -92$  °C (PB6407),<sup>13</sup> which is the closest

regular star structure available to these intermolecular clusters, and found close similarities even in the frequency breadth of the transition (see also discussion on Figure 3). (ii) The nearly molecular weight independent dynamic response of ZW2, which suggests the probing of primarily intramolecular dynamics, consistent with the network-like structure of these systems.<sup>3,9</sup> (iii) The large effect of molecular weight on ZW3 (ZW3-40 exceeds 3 decades).

Coming to Figure 1b, with increasing arm molecular weight the rubber plateau is also vastly extended to low frequencies, and the onset of the nearly parallel  $G'$  and  $G''$  behavior ( $G' \sim G'' \sim \omega^{0.4}$ ), reminiscent of the dynamic response of polymeric micronetworks,<sup>9</sup> is barely reached, but not the eventual flow regime (terminal slopes). The formed transient supramolecular networks are shown in the cartoon of Scheme 1b. Further, referring to Figure 1c, the simple Maxwellian dynamics detected in ZW3-15 cannot be captured at high molecular weights in the available experimental frequency window. In the limited frequency window available in the terminal region, there is evidence that  $G'$  and  $G''$  are nearly parallel, as in the case of ZW2 and microgel networks. This suggests that whereas for ZW3-15 the most probable form of self-organization is single spheres in equilibrium with a loose network of connected spheres (consistent with the SAXS data of ref 3), in the case of ZW3-40 the network dominates the response and is stronger and of larger scale (Figure 1c) with spheres still being possibly present (Scheme 1c); this is indirectly corroborated by the attempt to measure the structure of ZW3-40 with SAXS, indicating absence of structural peak in the  $q$  range available. We thus attribute the strong molecular weight effect to these spatially correlated soft spheres embedded in a network of interconnected stars, i.e., an analogy with the phase equilibria between small rings and reversible networks of finite density, predicted for solutions of associating telechelic polymers.<sup>5</sup> Similar conclusions hold for the other molecular weights measured (Table 1; see also discussion on ZW3-25 below).

Concerning the ZW3 sample, to test the stability of the proposed formation of collapsed star spherical configurations (which seem counterintuitive to a first approach, as it involves a large entropic penalty<sup>3</sup>), the effects of sample history on the dynamic response were examined. In particular, the star melts were prepared with three different protocols: (i) the as-synthesized samples were annealed for periods ranging from 12 h to 7 days, at 70 °C under vacuum; (ii) the melt samples were obtained through casting from dilute solution<sup>10</sup> in a solvent of reduced polarity (toluene) which does not favor the formation of clusters,<sup>6d</sup> and subsequently annealed as in (i), providing thus true equilibrium structures; and (iii) they were obtained through solution casting in a nonpolar solvent (cyclohexane) which favors aggregation and subsequently annealed as in (i). In all cases the results were identical, suggesting that within the experimental time and under these procedures the structures probed were stable.

For all systems investigated, the plateau modulus had virtually the same value of  $G_0 = 1.2 \times 10^6$  Pa within experimental error, indicating the same effective entanglement molecular weight.<sup>11,12</sup> For all stars, the (horizontal) shift factors  $a_T$  followed the well-known WLF behavior,<sup>12</sup>  $\log a_T = -C_1(T - T_r)/(C_2 + T - T_r)$ . The extracted WLF coefficients  $C_1$  and  $C_2$  were transformed into  $C_1^g$  and  $C_2^g$  at  $T_g$  according to<sup>12</sup>  $C_1^g = C_1 C_2 /$



**Table 2. WLF Constants for End-Functionalized Stars with Zwitterionic Groups Referred to Their Glass Transition Temperatures**

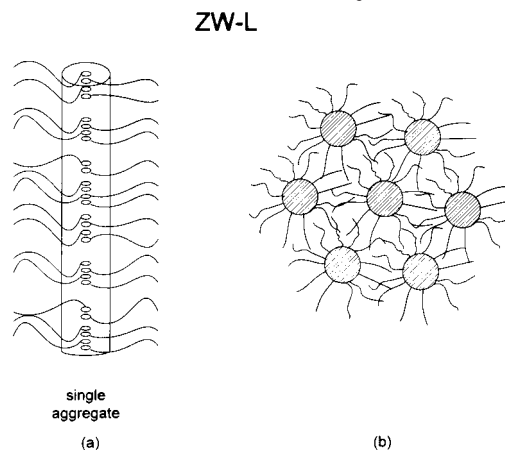
sample	$C_1^g$	$C_2^g$ (K)	sample	$C_1^g$	$C_2^g$ (K)
ZW1-15	11.4	47	ZW2-40	15.6	118
ZW2-15	10.1	66	ZW3-40	22.2	118
ZW3-15	14.4	93	star PB6407 <sup>a</sup>	10.6	38
ZW1-40	13.4	138	linear PB165 <sup>b</sup>	12	34

<sup>a</sup> Multiarm 1,4-polybutadiene star<sup>13</sup> with 64 arms and arm molecular weight  $M_a = 7000$  g/mol, used for comparison. <sup>b</sup> Linear 1,4-polybutadiene<sup>13</sup> with weight-average molecular weight  $M_w = 165\,000$  g/mol, used for comparison.

( $C_2 + T_g - T_r$ ) and  $C_2^g = C_2 + T_g - T_r$  and are listed in Table 2. It is apparent that for different molecular weights and degrees of functionalization there is a small difference in these values, attributed to the different structures; this finding is consistent with earlier  $C_1$  and  $C_2$  results on end-functionalized polyisoprenes.<sup>1b</sup> In systems without such structural differences (and no change in the chain microstructure) such as nonfunctionalized star polymers of different functionalities, the  $C_1$  and  $C_2$  values are virtually the same, irrespective of functionality or arm molecular weight.<sup>13</sup> For comparison, the respective values of the multiarm polybutadiene star PB6407,<sup>13</sup> as well as the linear polybutadiene PB165 with uniform chain microstructure and  $T_g = -96$  °C,<sup>13</sup> have been also included in Table 2. Their  $C_1^g$  and  $C_2^g$  values are within the universal range for homopolymers (8–18 for  $C_1^g$  and 30–70 for  $C_2^g$ ).<sup>12</sup> The close values of  $C_1^g$  and  $C_2^g$  for ZW1-15 (with  $f = 74^3$ ) and PB6407 are consistent with the suggested multiarm starlike self-organized structure of the former.<sup>3</sup>

An analysis of the ZW1 data suggests that a rough consideration of the arm relaxation process (which is independent of star functionality and thus of the aggregation number in this case), using the span molecular weight of the single star as an effective arm size, is only of qualitative value as a quantitative account of the measured times within the framework of tube theory for star arm relaxation is not possible.<sup>14</sup> This indicates that, given the dendrimeric structure of the monofunctionalized systems (Scheme 1a), the arm architecture plays an important role in the relaxation mechanism.<sup>15</sup> In addition, it is important to emphasize that these hyperstar structures may not be entirely spherical but rather represent distorted objects with disklike shape (reminiscent to some degree of comblike macromolecules forming cylindrical brushes<sup>16</sup>), as this shape is consistent with a linear antiparallel placement of the dipoles, which leads to the overall free energy minimization of the system.<sup>1c,6b,c,17</sup> It is actually expected that for low aggregation numbers (higher arm molecular weight of parent telechelic star) nearly spherical star structures are formed, whereas for high aggregation number (lower molecular weights) the structure resembles more like anisotropic discotic objects.<sup>1c,6b,c</sup>

The above discussion renders the investigation of the role of chain architecture (and thus the relevant self-organized structures) on the dynamics of telechelic polymers necessary. To address this issue, we used linear  $\omega$ -zwitterionic polybutadienes with only one end capped with zwitterionic groups (Table 1), in a range of molecular weights covering the stars arm molecular weights. These polymers order under the influence of intermolecular forces, forming tubular structures (for low molecular weights) or bcc lattices with long-range order (for high molecular weights).<sup>6b,c,17</sup> The cartoon of

**Scheme 2. Schematic Representation of the Self-Organization of the Linear One-End-Functionalized Polymers ZW-L<sup>a</sup>**

<sup>a</sup> (a) Single aggregate forming a tubular structure, illustrated by the drawn hypothetical cylinder. (b) Cross section of the ordered close-packed tubular aggregates.<sup>17</sup>

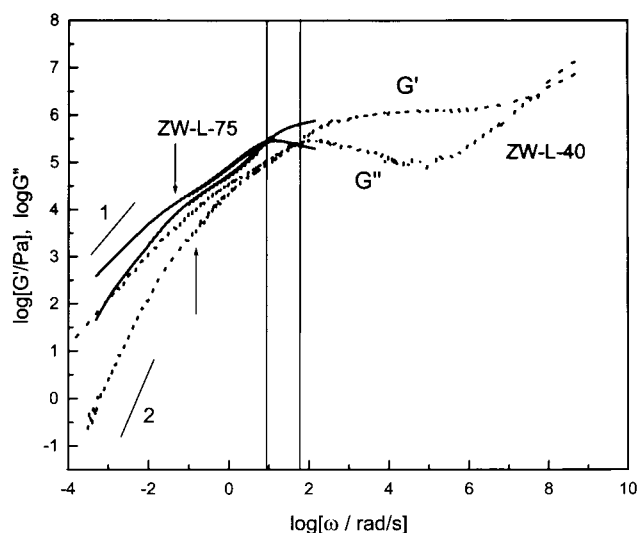


**Figure 2.** Master curves of storage ( $G'$ ) and loss ( $G''$ ) moduli at the reference temperature 27 °C for linear 1,4-polybutadiene ZW-L-40 (dotted lines) and ZW-L-75 (solid lines). The vertical lines indicate the crossover frequencies from rubber plateau to terminal relaxation, whereas the terminal slopes  $G' \sim \omega^2$  and  $G'' \sim \omega^1$  are also indicated. The vertical arrows indicate the onset of the slow relaxation mode.

Scheme 2 attempts to represent this type of supra-molecular self-assembly. Further, as seen in Figure 2, which depicts some typical linear viscoelastic data of ZW-L, their dynamics is characterized by a dual terminal relaxation behavior, with a fast mode relating to some kind of arm relaxation and a slow one to the overall structural reorganization of the clusters, qualitatively analogous to the behavior of other relevant ordered objects such as regular hyperstars,<sup>13</sup> ionomers,<sup>18</sup> and microgels;<sup>19</sup> in the present case, however, the interacting clusters are not spherical but cylindrical (Schemes 1 and 2).<sup>6,17,20</sup>

The relaxation times of all stars are compiled in the activation plot of Figure 3 and in Table 3.<sup>21</sup> In this figure, the arm relaxation (fast process) data from the nonionic multiarm polybutadiene stars with  $f = 64$  arms<sup>13</sup> are also included for comparison. The reasonable agreement of the multiarm stars with ZW1 supports the structural assignment of the latter for all molecular

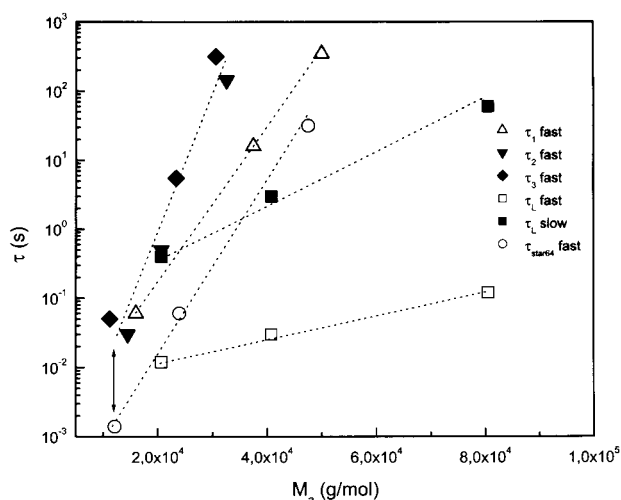


**Figure 3.** Compilation of the dynamic results for all telechelic 1,4-polybutadienes investigated in the form of a log-linear plot of terminal relaxation times versus arm molecular weight. The linear data are also included for comparison (see text). In this plot  $\tau$  refers to the terminal relaxation time; “fast” corresponds to the rubber–terminal transition, which relates to some kind of arm relaxation; “slow” refers to the longest relaxation time detected in the system (probably of structural origin; see text). Subscripts 1, 2, 3, and L refer to ZW1, ZW2, ZW3, and linear polymers, respectively;  $\tau_{\text{star64}}$  refers to relaxation times from nonionic multiarm polybutadiene stars with  $f = 64$ .<sup>13</sup>

**Table 3. Relaxation Times (in s) and Zero Shear Viscosities (in Pa·s) of the  $\omega$ -Functionalized Polybutadienes and Their Blends at  $T_r = 27^\circ\text{C}$**

sample	terminal $\tau_{\text{fast}}$	terminal $\tau_{\text{slow}}$	viscosity $\eta_0$
ZW1-15	0.06	0.224	250 000
ZW1-30	16	<i>a</i>	$> 3 \times 10^6$
ZW1-40	347	<i>a</i>	$> 10^7$
ZW2-15	0.03	75	195 000
ZW2-30	0.5	1333	600 000
ZW2-40	143	<i>a</i>	$> 10^7$
ZW3-15	0.05	<i>a</i>	45 000
ZW3-25	5.5	290	$4 \times 10^6$
ZW3-40	314	<i>a</i>	$> 10^8$
ZW-L-20	0.012	0.4	15 000
ZW-L-40	0.03	3	110 000
ZW-L-75	0.12	60	700 000
PB165	0.30	<i>a</i>	195 000
ZW3-15/PB165	0.22	<i>a</i>	130 000
$w_{\text{ZW3}} = 0.2$			
ZW3-15/PB165	0.23	<i>a</i>	120 000
$w_{\text{ZW3}} = 0.3$			
ZW3-15/PB165	0.17	<i>a</i>	73 000
$w_{\text{ZW3}} = 0.5$			
ZW3-15/ZW2-15	1.0	<i>a</i>	$> 75\,000$
$w_{\text{ZW3}} = 0.35$			
ZW3-15/ZW2-15	0.12	<i>a</i>	48 000
$w_{\text{ZW3}} = 0.53$			

<sup>a</sup> Experimentally inaccessible parameter.

weights. The quantitative differences between the ZW1-15 (with  $f = 74^3$ ) and the star with  $f = 64$  and nearly similar  $M_a \approx 14\,000$  g/mol point to the effect of the branched arm of the former on the relaxation, as already discussed (double arrow in Figure 3). Further, ZW2 and ZW3 exhibit similar dependence as ZW1 and the multiarm stars, but with nearly double activation barrier. Concerning the slow relaxations of the stars, as for the high molecular weights they cannot be detected within the experimental window available, they were not considered in Figure 3; only the linear ZW-L (tubular) slow modes are shown, exhibiting slightly stronger molecular weight dependence, as expected for structural

relaxation.<sup>13</sup> The large difference in the energetic barrier between linear and star telechelic polymers should relate to their pronounced structural differences discussed above. The measured relaxation times and zero-shear viscosities ( $\eta_0$ ) of the different star assemblies are summarized in Table 3. Note that whereas for ZW3-25 a slow process was detected, this was not the case neither for ZW3-40 (too slow to be detected, as discussed above) nor for ZW3-15. This observation corroborates the notion that the increase of arm molecular weight brings some changes in the ZW3 self-organization, as already mentioned. For lower arm molecular weight we have primarily collapsed soft-sphere configurations giving rise to one dominant relaxation mechanism, whereas with increasing arm molecular weight spheres of lower aggregation number (due to stereochemical reasons) are present and also participate in the formation of a reversible network, characterized by a dual terminal relaxation (Scheme 1c). Despite the lack of direct structural confirmation, this suggested mechanism of association provides a reasonable framework for explaining consistently all dynamic data and is further based on the available SAXS data on the ZW3-15 system.<sup>3</sup>

A useful test of the stability of the different structures and the potential to control the transition from one type of structure to another can be achieved through blending. To address this issue, we have employed the two mixtures ZW3-15/PB165 and ZW2-15/ZW3-15. As the zero-shear viscosity at the reference temperature of  $27^\circ\text{C}$  is nearly the same for PB165 and ZW2-15 (Table 3), the two blends have the same viscosity contrast but different structural features. In the former, we blend star forming predominantly collapsed soft-sphere configurations with nonionic linear chains, and the anticipated result is some kind of “dilution” of the structure and a rather weak penetration of the linear chains into the hyperstars. The much higher molecular weight of the nonfunctionalized linear chain compared to the star arms may create some kind of depletion layer around the supramolecular stars.<sup>22</sup> On the other hand, in the latter case we blend the soft-sphere objects with a strong apparently uncorrelated network, and depending on the relative amount of each constituent, we expect a diluted intermediate structure resembling either case. The results of the linear rheological investigations with the star/linear ZW3-15/PB165 mixture are summarized in Figure 4. It is evident that a smooth transition takes place from the dynamics (onset of terminal relaxation) of the one component (linear PB165, Figure 4a) to that of the other (ZW3-15, Figure 4e); this is seen as changes within the frequency region marked by the two vertical lines in Figure 4. Further, the terminal slopes have been reached at all compositions. On the basis of rheological (single relaxation process) as well as visual observations (samples remain clear and transparent at all times), all mixture compositions (Figure 4b–d) were homogeneous.<sup>23</sup>

Similar remarks hold for the star mixture ZW2-15/ZW3-15, which is now discussed referring to Figure 5. It is noted that the two components, each having entirely different structural organization, are homogeneously mixed in such a way that the transition from one component (ZW2-15, Figure 5a) to the other (ZW3-15, Figure 5d) is gradual. The mixture exhibits virtually branched network behavior at low ZW3-15 content with nearly parallel  $G'$  and  $G''$  (Figure 5b), which essentially

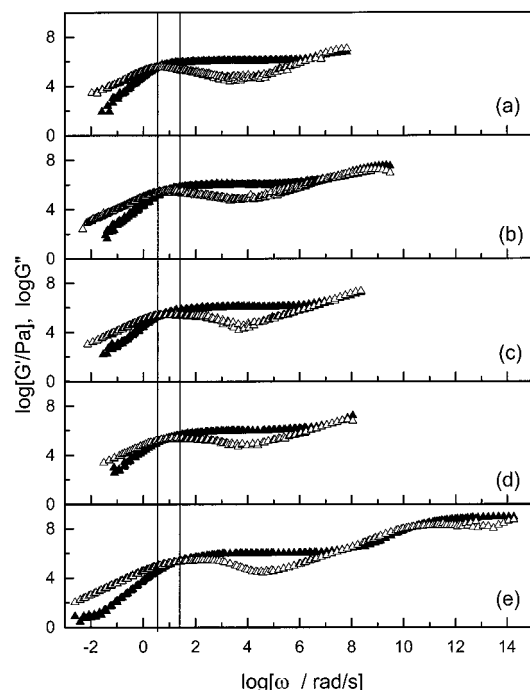


**Figure 4.** Linear viscoelastic response of star/linear mixtures ZW3-15/PB165. Master curves of  $G'$  ( $\blacktriangle$ ) and  $G''$  ( $\triangle$ ) at a reference temperature  $T_{\text{ref}} = 27^\circ\text{C}$ , at different compositions of ZW3-15 (mass fraction): (a) 0.00, (b) 0.20, (c) 0.30, (d) 0.50, and (e) 1.00. The vertical lines indicate the crossover frequencies from rubber plateau to terminal relaxation, for the PB165 (slower) and ZW3-15.

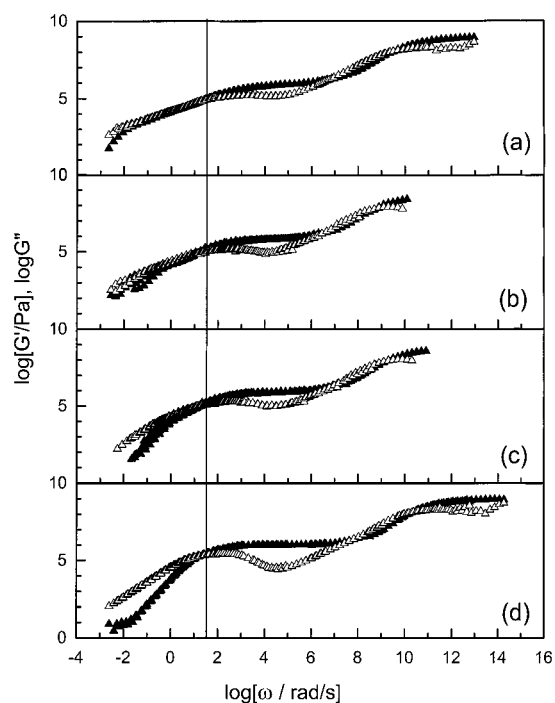


**Figure 5.** Linear viscoelastic response of star/star mixtures ZW3-15/ZW2-15. Master curves of  $G'$  ( $\blacktriangle$ ) and  $G''$  ( $\triangle$ ) at a reference temperature  $T_{\text{ref}} = 27^\circ\text{C}$ , at different compositions of ZW3-15 (mass fraction): (a) 0.00, (b) 0.35, (c) 0.53, and (d) 1.00. The vertical line indicates the crossover frequencies from rubber plateau to terminal relaxation, which for both components is virtually identical.

becomes weaker as the ZW3-15 composition increases (Figure 5c) and eventually is indistinguishable from the behavior of pure ZW3-15 at higher compositions, with the appropriate terminal slopes; the change of the latter

with composition is also evident. One should point out that identically the same behavior was observed irrespective of the use of solvent (toluene or cyclohexane) during preparation (see also Experimental Section), suggesting the strong equilibrium aggregation tendency of the stars into the above-mentioned supramolecular structures in the melt.<sup>3</sup> It is finally mentioned that for both mixtures of Figures 4 and 5 no clear SAXS pattern could be resolved at all compositions, apparently because the "dilution" effect of the linear PB165 (for Figure 4) or the ZW2-15 (in Figure 5) was such that the characteristic correlation lengths moved outside the detectable  $q$  range. Finally, the results of Figures 4 and 5 also support to assignment of different stable self-assemblies to ZW2-15 and ZW3-15 (Scheme 1).

#### 4. Concluding Remarks

The study of the linear viscoelastic properties of model mono-, di-, and tri- $\omega$ -functionalized three-arm star polybutadiene melts with zwitterionic end groups yielded the following conclusions. Depending on the degree of functionalization, these polymers can form distinctly different supramolecular structures, which however can be affected by the molecular weight, as it weakens the electrostatic interactions for stereochemical reasons. The dependence of the relaxation times of such macromolecular self-assemblies on the arm molecular weight indicates activated relaxation processes; the respective energetic barriers are much larger compared to those of end-functionalized linear chains, which form a range cluster structures from tubular to bcc and potentially networks with increasing molecular weight. Despite the absence of structural information for the high molecular weights, the investigation of melts prepared by different protocols, as well as of binary blends (star/linear and star/star), demonstrates the stability of the different self-organized structures and provides a means to control structural transitions in this type of systems.

**Acknowledgment.** We are grateful to T. Pakula for helpful discussions and the SAXS studies and to J. Roovers for providing the linear PB165 sample.

#### References and Notes

- (1) Young, R. N.; Quirk, R. P.; Fetters, L. J. *Adv. Polym. Sci.* **1984**, *56*, 1. Fetters, L. J.; Graessley, W. W.; Hadjichristidis, N.; Kiss, A. D.; Pearson, D. S.; Younghouse, L. B. *Macromolecules* **1988**, *21*, 1644. Hadjichristidis, N.; Pispas, S.; Pitsikalis, M. *Prog. Polym. Sci.* **1999**, *24*, 875.
- (2) Muthukumar, M.; Ober, C. K.; Thomas, E. L. *Science* **1997**, *277*, 1225. Zimmerman, S. C.; Zheng, F.; Reichert, D. E. C.; Kolotuchin, S. V. *Science* **1996**, *271*, 1095. McLeish, T. C. B., Ed.; *Theoretical Challenges in the Dynamics of Complex Fluids*; NATO ASI Vol. 339; Kluwer: London, 1997.
- (3) Vlassopoulos, D.; Pakula, T.; Fytas, G.; Pitsikalis, M.; Hadjichristidis, N. *J. Chem. Phys.* **1999**, *111*, 1760.
- (4) Pitsikalis, M.; Hadjichristidis, N. *Macromolecules* **1995**, *28*, 3904.
- (5) Semenov, A. N.; Nyrkova, I. A.; Cates, M. E. *Macromolecules* **1995**, *28*, 7879.
- (6) Pitsikalis, M.; Hadjichristidis, N.; Mays, J. W. *Macromolecules* **1996**, *29*, 179. Pitsikalis, M.; Siakali-Kioulafa, E.; Hadjichristidis, N. *J. Polym. Sci., Part B: Polym. Phys.* **1996**, *34*, 244. Pitsikalis, M. Ph.D. Dissertation, University of Athens, 1994. Siqueira, D. F.; Pitsikalis, M.; Hadjichristidis, N.; Stamm, M. *Langmuir* **1996**, *12*, 1631.
- (7) Semenov, A. N.; Rubinstein, M. *Macromolecules* **1998**, *31*, 1373.
- (8) It is also noted that concerning ZW1, the slow terminal relaxation, attributed to structural rearrangements of the self-organized hyperstar structures (ref 3) and detected rheologically only in ZW1-15, is strongly strain dependent;

this suggests a rather delicate and easily disrupted structure, in harmony with earlier findings (ref 1b). However, these types of structures are also characterized by a remarkable thermal stability of the zwitterionic interactions (ref 3).

- (9) Antonietti, M.; Fölsch, K. J.; Sillescu, H.; Pakula, T. *Macromolecules* **1989**, *22*, 2812.
- (10) The melts were obtained from the homogeneous solutions by slowly evaporating the solvent over the course of 3 days under vacuum at room temperature (25 °C).
- (11) From  $G_0 = 4/5\rho RT/M_e$ ,  $M_e$  is estimated to be around 2000 g/mol, which is very reasonable for polybutadiene.
- (12) Ferry, J. D. *Viscoelastic Properties of Polymers*, 3rd ed.; Wiley: New York, 1980.
- (13) Vlassopoulos, D.; Pakula, T.; Fytas, G.; Roovers, J.; Karatasos, K.; Hadjichristidis, N. *Europhys. Lett.* **1997**, *39*, 617. Pakula, T.; Vlassopoulos, D.; Fytas, G.; Roovers, J. *Macromolecules* **1998**, *31*, 8931. Kapnistos, M.; Semenov, A. N.; Vlassopoulos, D.; Roovers, J. *J. Chem. Phys.* **1999**, *111*, 1753.
- (14) McLeish, T. C. B.; Milner, S. T. *Adv. Polym. Sci.* **1999**, *143*, 195.
- (15) Such an idea is currently being considered theoretically, in treelike low functionality star polymers for different applications, resembling however the hyperbranched assemblies of ZW1 (McLeish, T. C. B., personal communication, 1999).
- (16) Saariaho, M.; Subbotin, A.; Ikkala, O.; tenBrinke, G. *Macromol. Rapid Commun.* **2000**, *21*, 110. Vlassopoulos, D.; Fytas, G.; Loppinet, B.; Isel, F.; Lutz, P. J.; Benoit, H. *Macromolecules* **2000**, *33*, 5960.
- (17) Shen, Y.; Safinya, C. R.; Fetters, L. J.; Adam, M.; Witten, T.; Hadjichristidis, N. *Phys. Rev. A* **1991**, *43*, 1886.
- (18) Séréto, Y.; Aznar, R.; Porte, G.; Berret, J.-F.; Calvet, D.; Collet, A.; Viguier, M. *Phys. Rev. Lett.* **1998**, *81*, 5584. Weiss, R. A.; Fitzgerald, J. J.; Kim, D. *Macromolecules* **1991**, *24*, 1071. Kim, J.-S.; Yoshikawa, K.; Eisenberg, A. *Macromolecules* **1994**, *27*, 6347.
- (19) Antonietti, M.; Pakula, T.; Bremser, W. *Macromolecules* **1995**, *28*, 4227.
- (20) Because of the high molecular weights, the linear chains were not appropriate for SAXS measurements in order to obtain direct structural information from the present ZW-L samples.
- (21) It is noted that a more accurate consideration of the change in relaxation times is normally made under isofriction conditions, i.e., by using the normalized (to the segmental) relaxation time in order to correct for the differences in the  $T_g$ 's (Table 1); because of the limited segmental data available, this was not possible for all samples investigated. However, the qualitative trends discussed in this work remain unchanged, as demonstrated for the cases where the segmental time is available (Table 3).
- (22) Watanabe, H. *Acta Polym.* **1997**, *48*, 215. Vlassopoulos, D.; Fytas, G.; Roovers, J.; Pakula, T.; Fleischer, G. *Faraday Discuss.* **1999**, *112*, 225. Gohr, K.; Pakula, T.; Tsutsumi, K.; Schärfl, W. *Macromolecules* **1999**, *32*, 7156.
- (23) Huh, J.; tenBrinke, G. *J. Chem. Phys.* **1998**, *109*, 789.

MA000741K